

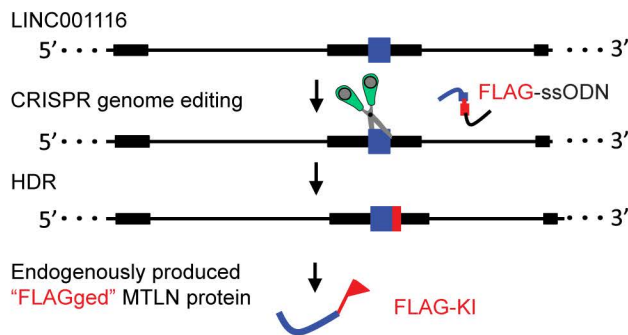
**Stem Cell Reports, Volume 14**

**Supplemental Information**

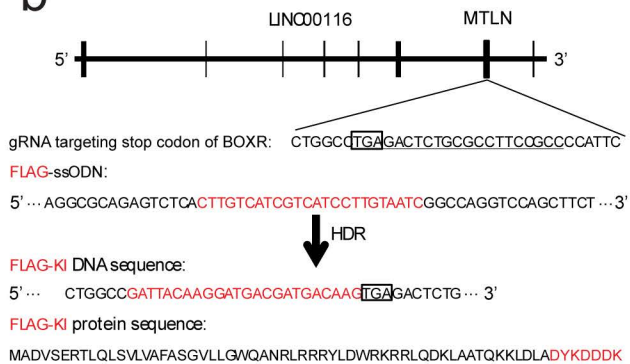
**Mitoregulin Controls  $\beta$ -Oxidation in Human and Mouse Adipocytes**

**Max Friesen, Curtis R. Warren, Haojie Yu, Takafumi Toyohara, Qiurong Ding, Mary H.C. Florido, Carolyn Sayre, Benjamin D. Pope, Loyal A. Goff, John L. Rinn, and Chad A. Cowan**

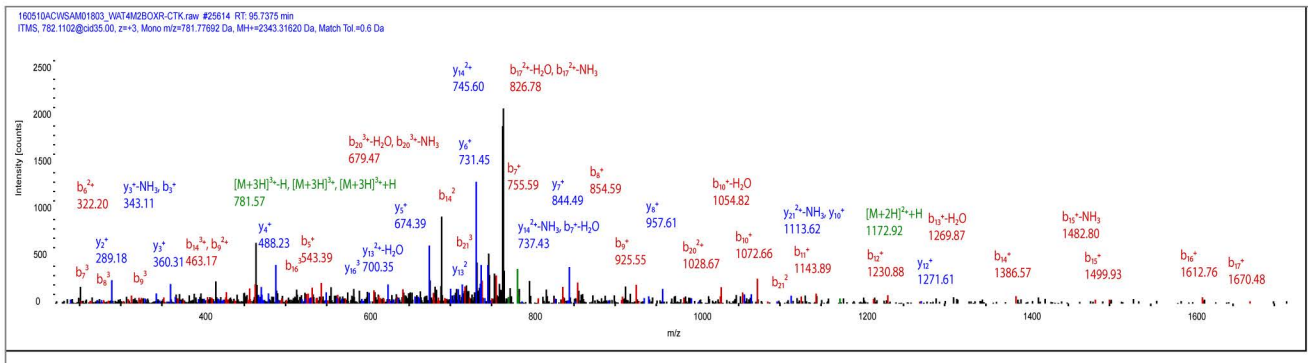
a



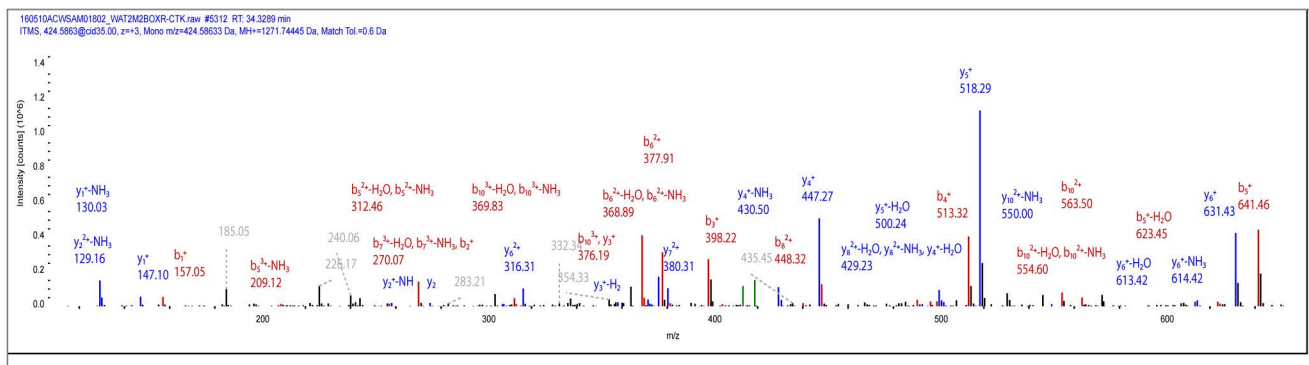
b



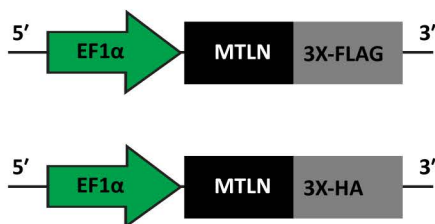
c



d



e



f

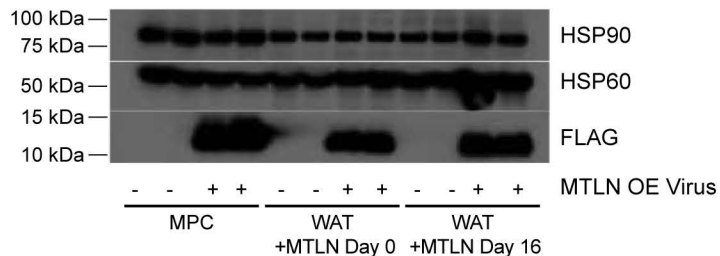


Figure S2 a

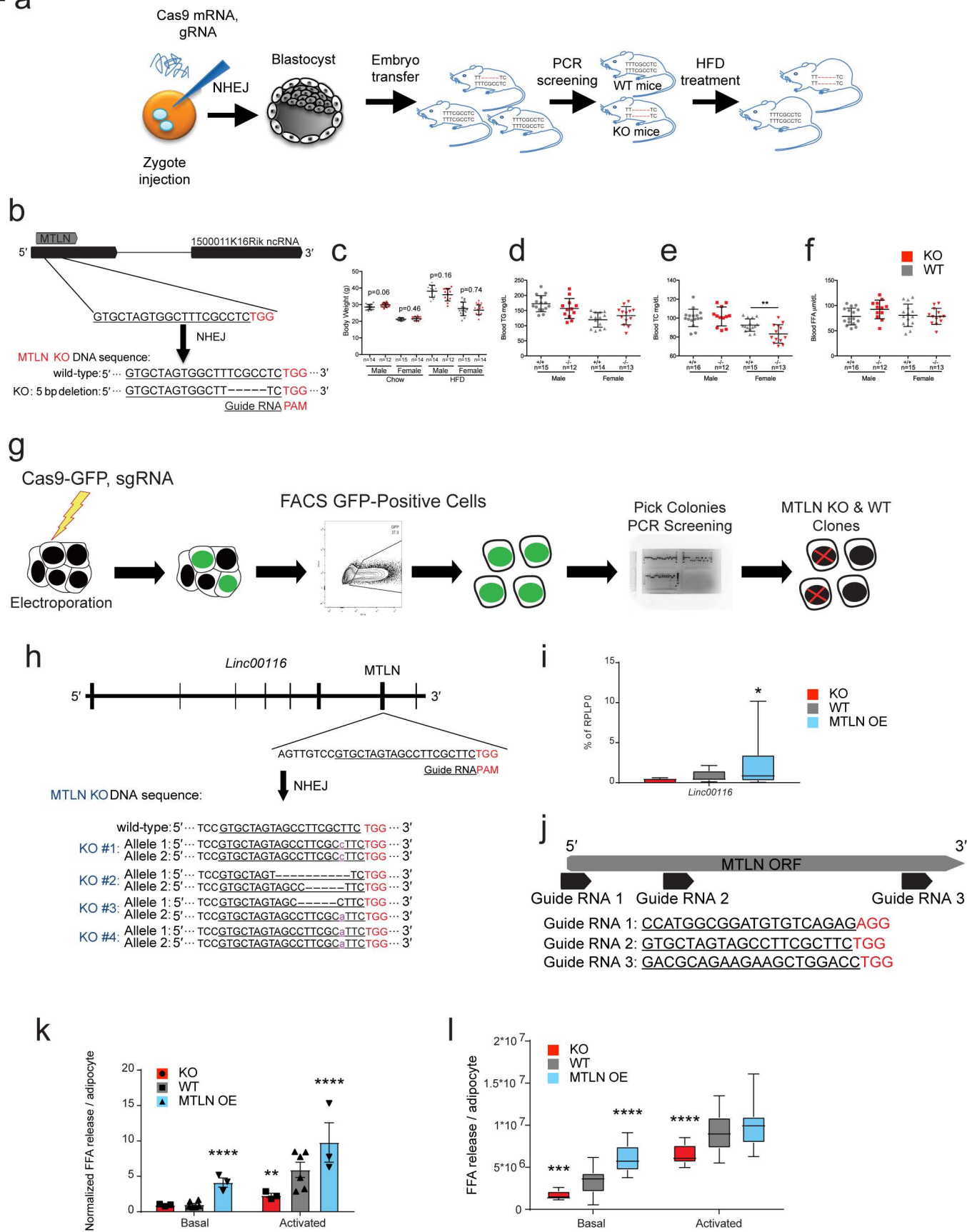
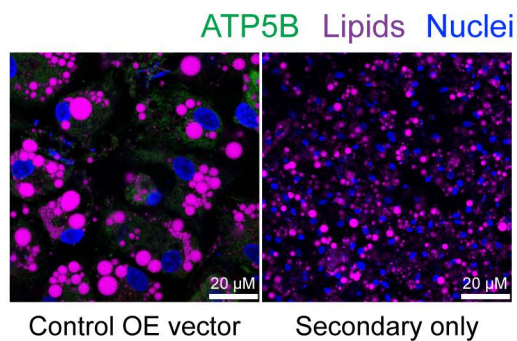
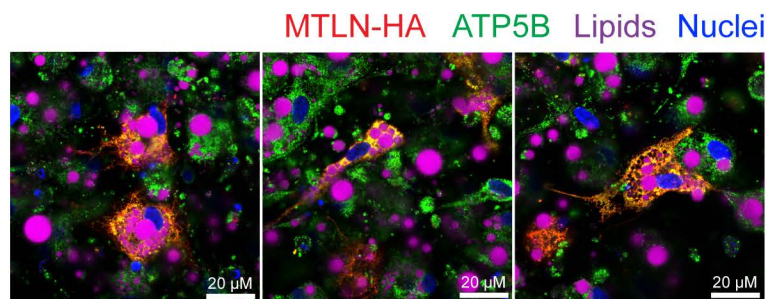


Figure S3

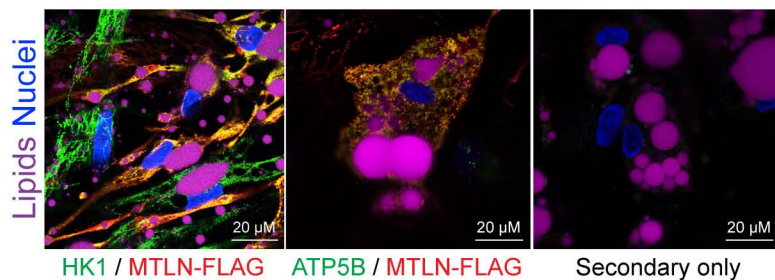
a



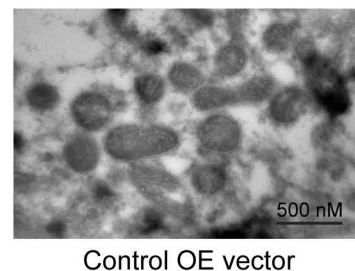
b



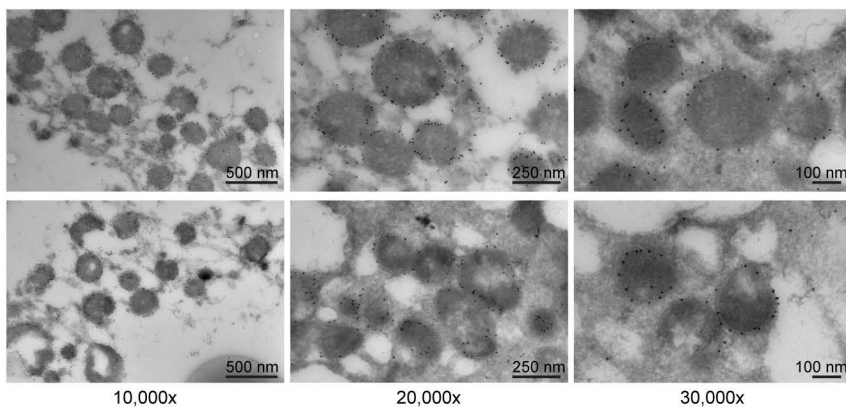
c



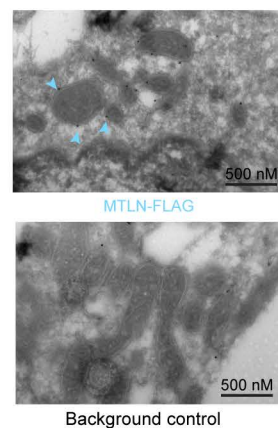
d



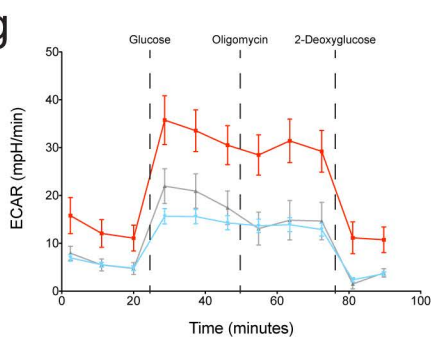
e



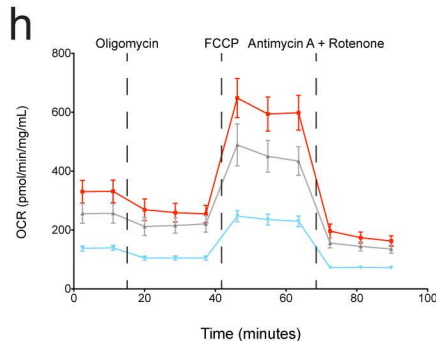
f



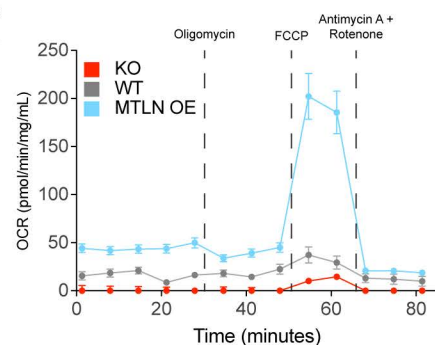
g



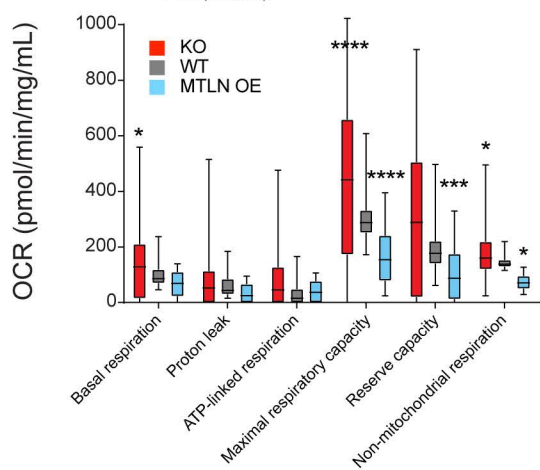
h



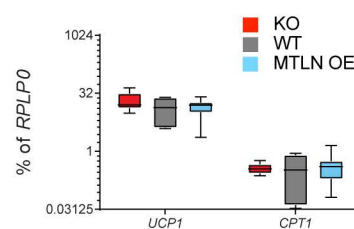
i



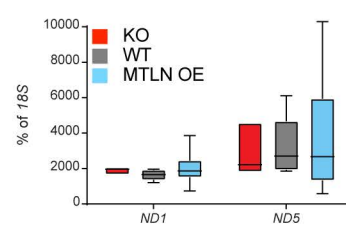
j



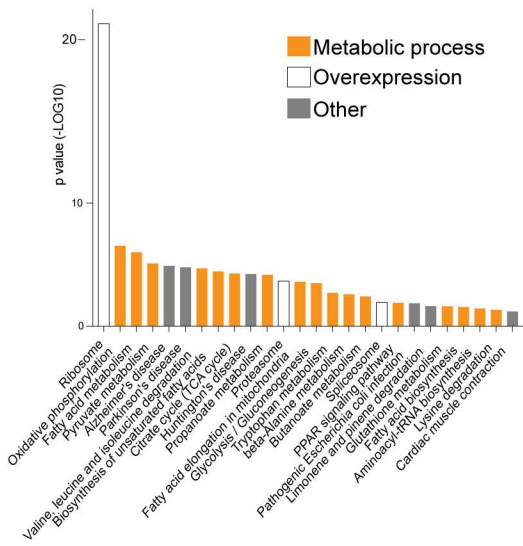
k



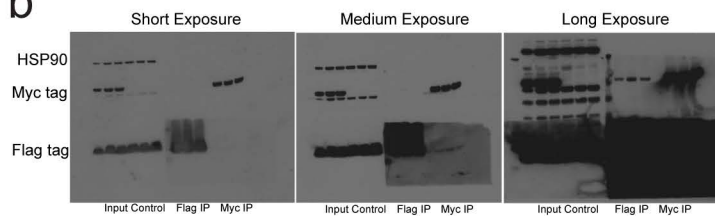
l



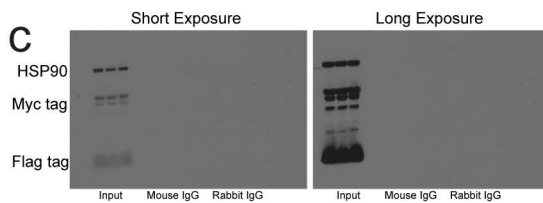
a



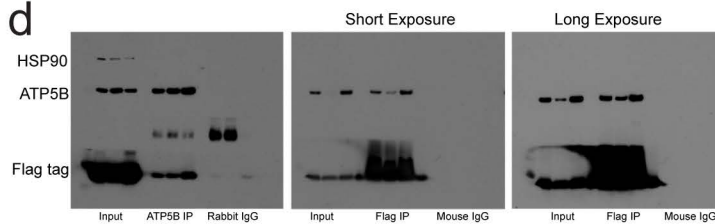
b



c



d





**Supplemental Figure 1. MTLN-Flag methodology, related to Figure 1.** a) Schematic of the experimental procedure for knocking in a FLAG-tag at the c-terminus of MTLN in hPSCs. b) Partial sequence of the MTLN smORF, FLAG knock-in ssODN, and guide RNA used to generate knock-ins. The resultant DNA and peptide sequence after genome editing is also shown. c) Mass spectrometry spectrum identifying the 2.34 kDa peptide of MTLN. d) Mass spectrometry spectrum identifying the 1.27 kDa peptide of MTLN. e) Schematic of the MTLN-FLAG and MTLN-HA expression constructs inserted into a lentiviral packaging vector. f) Immunoblot demonstrating overexpression of lentiviral MTLN-FLAG in MPCs, MPCs differentiated into hPSC-adipocytes (WAT), or hPSC-adipocytes transduced with MTLN-FLAG after differentiation (WAT+MTLN Day 16).

**Supplemental Figure 2. Supplemental data describing mouse and *in vitro* models of MTLN function, related to Figure 2.** a) Experimental design for the creation of MTLN<sup>-/-</sup> mice and HFD treatment. b) Schematic of the murine *1500011K16Rik* ncRNA gene and MTLN smORF. The guide RNA is underlined, the protospacer-adjacent motif (PAM) is in red. Knockout mutation sequence indicated below. c) Body weight of mice on chow or HFD (10.5 weeks). d-f) Serum concentrations of TG (d), total cholesterol (e), and FFA (f) on chow diet. g) Experimental design for knocking out MTLN in hPSCs. h) Schematic of the human *LINC00116* gene and MTLN smORF. The guide RNA is underlined, the PAM is in red. Knockout line indel sequences indicated below. i) qRT-PCR analysis of *MTLN* expression in differentiated hPSC-adipocytes. n=18 for WT, 30 for KO, 48 for OE. j) Pool of guide RNA sequences used in SGBS knockout experiments. k) Concentration of FFAs released into the medium of differentiated murine pre-adipocytes under basal or forskolin stimulated conditions. n=6 for WT, 3 for KO and OE. l) Concentration of FFAs released into the medium of hPSC-adipocytes under basal or forskolin stimulated conditions. n=30/21 for WT, 42/42 for KO, 66/90 for OE basal/stimulated. Data are means ± SD. \* = p ≤ 0.05, \*\* = p ≤ 0.01, \*\*\* = p ≤ 0.001, \*\*\*\* = p ≤ 0.0001, one- or two-way ANOVA. All n's are independent biological replicates performed in technical duplicate.

**Supplemental Figure 3. Extended data related to subcellular localization and energetic effects of MTLN, related to Figure 3.**

a) Confocal microscopy depicting ATP5B (green), neutral lipids (pink), and nuclei (blue) in hPSC-adipocytes. The left panel is an exposure-matched control OE vector as a negative control indicating HA antibody background staining. The right panel is an exposure-matched secondary antibody-only image as a negative control indicating background fluorescence. Scale bar, 20  $\mu$ m. b) Confocal microscopy showing MTLN-HA (red), ATP5B (green), neutral lipids (purple), and nuclei (blue) in differentiated hPSC-adipocytes in triplicate replicating experiments. Scale bar, 20  $\mu$ m. c) Confocal microscopy showing MTLN-FLAG (red), HK1/ATP5B (green), neutral lipids (purple), and nuclei (blue) in hPSC-adipocytes. The right panel is an exposure-matched secondary antibody-only image as a negative control indicating background fluorescence. Scale bar, 20  $\mu$ m. d) Anti-HA immunogold-labeled hPSC-adipocytes with a control OE vector serves as a negative control for transmission electron microscopy studies. e) Immunogold labeling of MTLN-HA in differentiated hPSC-adipocytes. Replicate experiments at three magnification levels are shown. f) Immunogold labeling of MTLN-FLAG in differentiated hPSC-adipocytes. Arrows point to gold particles localized at the mitochondrial membrane. g) ECAR of hPSC-adipocytes during serial stimulation with glucose, oligomycin, and 2-deoxyglucose. n=30. h) OCR of hPSC-adipocytes during serial stimulation with oligomycin, CCCP, and antimycin A/rotenone. n=30. i) OCR of hPSC-adipocytes during starvation followed by serial stimulation with palmitate, oligomycin, CCCP, and antimycin A/rotenone. n=35. j) Comparison of basal and ATP-linked respiration, as well as maximal and spare respiratory capacity of hPSC-adipocytes. n=30. k) *UCP1* and *CPT1* mRNA expression analysis of MTLN KO, WT, and MTLN OE hPSC-adipocytes. n=9. l) *ND1* and *ND5* mtDNA quantity analysis of MTLN KO, WT and MTLN OE hPSC-adipocytes. n=6 for WT and KO, 9 for OE. Data are means  $\pm$  SD. \* =  $p \leq 0.05$ , \*\* =  $p \leq 0.01$ , \*\*\* =  $p \leq 0.001$ , one- or two-way ANOVA. All n's are independent biological replicates performed in technical duplicate.

**Supplemental Figure 4. Extended data related to biological pathway analysis and MTLN interactions, related to Figure 4.** a) Gene ontology analysis describing the biological pathways enriched in the co-immunoprecipitated proteins bound to MTLN-Flag. Orange: mitochondrial processes. White: protein translation and overexpression. Grey: Other. Modified Fisher Exact P-Value, EASE Score. Data in Supplemental Table 4. b-d) uncropped immunoblots used in Figure 4.



Supplemental Table 4. Kegg Pathway Analysis of Immunoprecipitated Proteins, Related to Supplementary Figure 4a.

<b>Term</b>	<b>PValue</b>	<b>FDR</b>
<b>Ribosome</b>	2.81E-25	3.29E-22
<b>Oxidative phosphorylation</b>	2.94E-07	3.43E-04
<b>Fatty acid metabolism</b>	1.01E-06	0.001177483
<b>Pyruvate metabolism</b>	8.15E-06	0.009534287
<b>Alzheimer's disease</b>	1.26E-05	0.014744305
<b>Parkinson's disease</b>	1.61E-05	0.01885183
<b>Valine, leucine and isoleucine degradation</b>	2.03E-05	0.023750611
<b>Biosynthesis of unsaturated fatty acids</b>	3.56E-05	0.041635892
<b>Citrate cycle (TCA cycle)</b>	5.27E-05	0.061626906
<b>Huntington's disease</b>	5.76E-05	0.067281384
<b>Propanoate metabolism</b>	6.76E-05	0.078968375
<b>Proteasome</b>	2.19E-04	0.255326078
<b>Fatty acid elongation in mitochondria</b>	2.56E-04	0.298580235
<b>Glycolysis / Gluconeogenesis</b>	3.24E-04	0.378657897
<b>Tryptophan metabolism</b>	0.001928104	2.231394172
<b>beta-Alanine metabolism</b>	0.002633853	3.03670699
<b>Butanoate metabolism</b>	0.003878293	4.441943803
<b>Spliceosome</b>	0.011819171	12.97912799
<b>PPAR signaling pathway</b>	0.012556727	13.73555596
<b>Pathogenic Escherichia coli infection</b>	0.014189132	15.38839481
<b>Limonene and pinene degradation</b>	0.023492963	24.26852227
<b>Glutathione metabolism</b>	0.025034765	25.65491006
<b>Fatty acid biosynthesis</b>	0.027528922	27.84859109
<b>Aminoacyl-tRNA biosynthesis</b>	0.037197044	35.80420646
<b>Lysine degradation</b>	0.048336348	43.97110827
<b>Cardiac muscle contraction</b>	0.063839579	53.76136456